Presented at the 1995 IEEE Workshop on Nonlinear Signal & Image Processing
Neos Marmaras-Halkidiki, Greece, June 20-22, 1995. Published in the Conference Proceedings

Multi-Component Signal Demodulation and Reconstruction Using AM-FM Modulation Models *

Joseph P. Havlicek, David S. Harding, and Alan C. Bovik
Laboratory for Vision Systems, University of Texas, Austin, TX 78712-1084, USA

ABSTRACT — **We model nonstationary, locally-coherent signals with multi-component AM-FM functions. Signal components are isolated by a multiband bank of Gabor wavelets, and estimates of the modulating functions are derived from each channel using a localized, computationally efficient nonlinear algorithm. In computing the multi-component AM-FM representation, Kalman filters are used to track each identified component across the filterbank channel responses. For the first time, we also demonstrate reconstruction of a complicated signal from the estimated modulating functions.**

1 Introduction

The treatment of wideband, nonstationary signals is important in a wide variety of applications including speech, audio, radar, and sonar signal processing. Often the signals of interest can be decomposed into a sum of several components that are each *narrowband* on a local scale, or *locally coherent*, where the information is manifest. In analyzing and interpreting such multi-component signals, it is desirable to characterize the structure of each component on a spectro-temporally localized basis; instantaneous frequency analysis is but one example. Computationally efficient AM-FM modeling techniques, which are inherently capable of capturing and representing local nonstationarities, have been the subject of significant recent interest [1-9]. Maragos, Quatieri, and Kaiser [1,3,6,7] and Bovik, Maragos, and Quatieri [5,8] characterized and popularized the *Teager-Kaiser Energy Operator* for AM-FM signal demodulation. Bovik, *et. al.,* demonstrated powerful characterizations of images in terms of amplitude and frequency modulation models [2]. Havlicek, Bovik, and Maragos introduced a related demodulation algorithm unique in its ability to estimate instantaneous frequency with correct sign information [4], and Havlicek and Bovik combined this algorithm with component tracking to extend the analysis to multi-component images [9].

In this paper we develop powerful new nonlinear techniques for simultaneously estimating the modulating functions associated with each of the multiple components comprising a multi-partite nonstationary signal $t(x)$ modeled as

$$t(x) = \sum_{k=1}^{K} a_k(x) \exp\left[j\varphi_k(x)\right], \qquad (1)$$

where $x \in \mathbb{R}$, $t : \mathbb{R} \to \mathbb{C}$, $a : \mathbb{R} \to [0, \infty)$, and $\varphi : \mathbb{R} \to \mathbb{R}$. For the first time, we also demonstrate reconstruction of a signal from the multi-component AM-FM representation.

2 Nonlinear Demodulation Algorithm

For a single nonstationary complex valued signal component

$$t(x) = a(x) \exp\left[j\varphi(x)\right], \qquad (2)$$

the demodulation problem involves estimating the amplitude envelope $a(x)$ and instantaneous frequency $\omega(x) = \frac{\mathrm{d}}{\mathrm{d}x}\varphi(x) = \varphi'(x)$ that characterize the local signal structure. Observing that

$$t'(x) = jt(x)\varphi'(x) + \exp\left[j\varphi(x)\right] a'(x) \qquad (3)$$

immediately leads to the nonlinear demodulation algorithm

$$a(x) = |a(x)| = |t(x)| = |a(x) \exp\left[j\varphi(x)\right]|, \quad (4)$$

and

$$\omega(x) = \mathrm{Re}\left[\frac{t'(x)}{jt(x)}\right]. \qquad (5)$$

If the signal of interest is real, we form the associated complex analytic signal by adding j times its Hilbert transform prior to demodulation [10].

*This research was supported in part by a grant from the Texas Advanced Research Projects Agency and by the Air Force Office of Scientific Research, Air Force Systems Command, USAF, under grant number F49620-93-1-0307.

3 Multi-Component Demodulation

Since the demodulation algorithm (4),(5) is nonlinear, it breaks down in the presence of out-of-band additive noise or multiple components due to cross-term interference [8]. In these situations it is necessary to *isolate* the various components prior to demodulation by processing the signal with a multiband bank of Gabor filters, which are optimal in their conjoint time-frequency uncertainty [2]. This scheme isolates the AM-FM components on a temporally local basis, and we subsequently apply the demodulation algorithm to the filtered channel outputs, with the modification that the filtered amplitude estimates must be divided by the appropriate channel filter magnitude evaluated at the estimated instantaneous frequency. While this *filtered* demodulation scheme is only approximate, the approximation error is tightly bounded, provided the filterbank is designed prudently [4].

3.1 Filter Bank

All of the filters have unit L^2 norm in both domains to preserve the signal energy in each filter passband. The equation for a filter with center frequency f_m is

$$g_m(x) = \frac{1}{\sqrt[4]{2\pi\sigma_m^2}} \exp\left[\frac{-x^2}{4\sigma_m^2}\right] \exp\left[j2\pi f_m x\right],$$

with Fourier transform

$$G_m(f) = \sqrt[4]{8\pi\sigma_m^2} \exp\left[-4\pi^2\sigma_m^2(f-f_m)^2\right].$$

With $\gamma = (2^{\mathrm{B}}-1)^2/(2^{\mathrm{B}}+1)^2$, we take $\sigma_m = \sqrt{-\ln\eta}/(2\pi\gamma f_m)$ so that each filter has an η-peak bandwidth of B octaves. The filter center frequencies progress geometrically with common ratio 2^B, such that the center frequencies of adjacent filters are related by $f_{m+1} = 2^B f_m$. This arrangement ensures that adjacent filters intersect precisely where each is at a fraction η of peak response.

We use a bank of $M+1$ filters, and f_0, the center frequency of the initial filter, is a design parameter. This places the center frequency of the final filter at $f_M = 2^{MB} f_0$. The filter tesselation covers every point in the frequency domain from B octaves below f_0 to B octaves above f_M with a filter that is responding at a fraction η or greater of it's peak response. For the examples in this paper, we used a bank of half-octave filters intersecting at half-peak, giving $\eta = B = \frac{1}{2}$. The discrete frequency representation of the filterbank is shown in Figure 1.

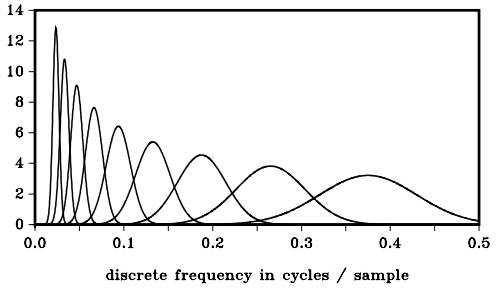

Figure 1: Discrete frequency representation of the filterbank. The filter spectra are positive and real valued.

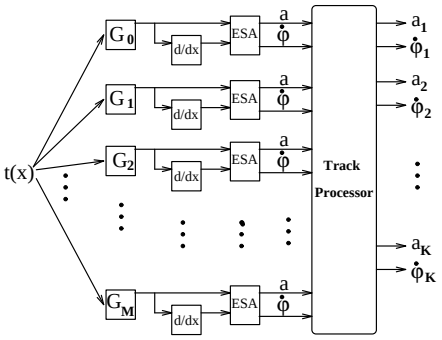

Figure 2: Block diagram of the multi-component algorithm.

3.2 Tracking of Multiple Components

With the filtered demodulation algorithm, every channel in the multiband filter bank produces observations of $a(x)$ and of $\omega(x)$ at every point in the domain of the signal. The problem of multi-component demodulation then becomes one of determining which channel should be used in estimating the modulating functions of *each* component at each point.

Suppose two components exist in a region of the domain of the signal. If we traverse the domain points in order, the instantaneous frequency of each component maps out a track in the frequency domain. At each point, we decide which channel to use in estimating the modulating functions of a given component by following that component's frequency domain track with a track processor. A block diagram of the overall scheme is shown in Figure 2. The filtered demodulation algorithm is performed in the blocks marked "ESA".

For each identified signal component, $a(x)$ and

$\omega(x)$ are tracked. We make no specific assumptions about statistical correlation between these quantities, and track each separately. Here, we present only the equations for tracking $\omega(x)$; the track filter for $a(x)$ differs only in it's Kalman gain sequences. First, write ω_k, the samples of $\omega(x)$, in a first order Taylor series:

$$\omega_k = \omega_{k-1} + \omega'_{k-1} + \int_{k-1}^{k} (k-t)\omega''(t)dt. \quad (6)$$

Since each signal component is locally-coherent, ω_k should not vary too rapidly or too wildly from sample to sample. Hence, we do not model the higher order terms of the series explicitly, but rather consider that ω' is essentially a constant plus a drift, where the drift is an uncorrelated noise process u_k. This immediately gives the simple and widely applicable plant model

$$\begin{bmatrix} \omega_{k+1} \\ \omega'_{k+1} \end{bmatrix} = \begin{bmatrix} 1 & 1 \\ 0 & 1 \end{bmatrix} \begin{bmatrix} \omega_k \\ \omega'_k \end{bmatrix} + \begin{bmatrix} 0 \\ 1 \end{bmatrix} u_k. \quad (7)$$

The design of an elegant Kalman track filter involving only *scalar* equations is straightforward from the model (7):

$$\widehat{\omega}_{k|k} = \widehat{\omega}_{k|k-1} + \alpha_k(\omega^o_k - \widehat{\omega}_{k|k-1}) \quad (8)$$

$$\widehat{\omega'}_{k+1|k} = \widehat{\omega'}_{k|k-1} + \beta_k(\omega^o_k - \widehat{\omega}_{k|k-1}) \quad (9)$$

$$\widehat{\omega}_{k+1|k} = \widehat{\omega}_{k|k} + \widehat{\omega'}_{k+1|k}, \quad (10)$$

where α_k and β_k are the Kalman gain sequences, ω^o_k is the observation of ω at sample k derived from the channel whose center frequency is closest to $\widehat{\omega}_{k|k-1}$ in units of σ_m^{-1}, $\widehat{\omega}_{k|k-1}$ is the prediction of ω at sample k given $k-1$ observations, and $\widehat{\omega}_{k|k}$ is the estimate of ω at sample k given k observations. The observation a^o_k used to update the amplitude track filter for a component is *always* taken from the same channel as ω^o_k.

3.2.1 New Track Starts

We consider starting a new track on any channel that produces a large amplitude observation a^o_k, and whose frequency observation ω^o_k does not lie too close to the predicted frequency of an existing track. However, our confidence in the observations produced by a channel is highest when the observed frequency is close to the channel center frequency, since this generally affords improved immunity against out-of-band information through an enhanced SNR. The quantity $\left|G_m(\frac{1}{2\pi}\omega)\right| / \max_f |G_m(f)|$ lies between zero and one, and increases as ω moves closer to the filter center frequency. Hence we define the *quality* of channel m at each point k by

$$Q_{k,m} = \frac{a^o_{k,m}\left|G_m(\frac{1}{2\pi}\omega^o_{k,m})\right|}{\max_f |G_m(f)|}, \quad (11)$$

where $a^o_{k,m}$ and $\omega^o_{k,m}$ are the amplitude and frequency estimates produced by channel m at the point k, respectively.

At each sample, we start new tracks on the channels with the highest values of $Q_{k,m}$, provided that $\omega^o_{k,m}$ does not lie in the η-peak passband of a channel that was used to update an already existing track at k.

4 Reconstruction

Reconstructing a component of the signal from the discrete AM-FM representation $a(x)$, $\omega(x)$ is an overdetermined problem. Given as an initial condition one complex valued sample obtained from the channel filter used to estimate the component's instantaneous amplitude and frequency, the instantaneous phase $\varphi(x)$ can be reconstructed by simply summing the frequency estimates. The component can then be reconstructed by substituting the amplitude estimates and reconstruction of $\varphi(x)$ directly into the model (2).

In practice, however, the frequency estimates will contain errors which arise from the approximation inherent in the filtered demodulation algorithm, as well as from cross-component interference. The deleterious effects of these errors on the reconstructed component would be cumulative if only a single initial condition were used.

Instead, we divide the portion of the domain where a component is supported into several disjoint segments and perform the reconstruction independently over each segment. This requires incorporating an initial condition for *each* segment into the AM-FM representation of *each* component. Finally, the multi-partite signal $t(x)$ is reconstructed by summing the individually reconstructed components, according to the model (1).

5 Example

Figure 3 shows an example of reconstructing a two-component signal from the estimated modulating functions. The original signal, shown in the (a) part of the figure, is the sum of two linear chirps with Gaussian amplitude modulation. The frequency of the first component varies from 0.0347 to 0.0893 Hz/sample, while that of the second component varies from 0.381 to 0.271 Hz/sample. The Gaussian space constants for the

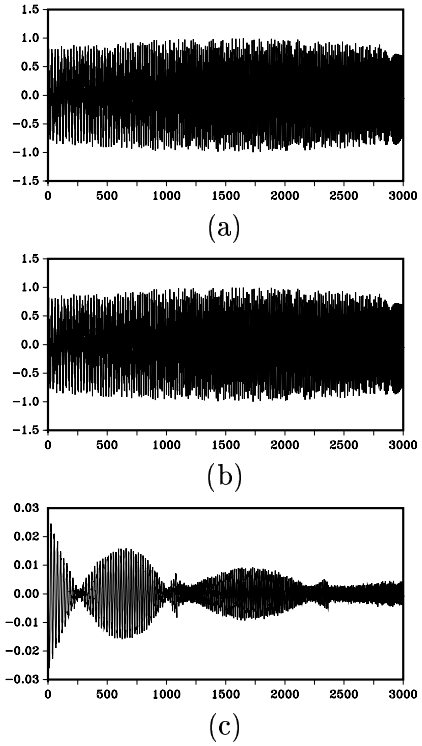

Figure 3: Two-component example: (a) original signal, (b) reconstructed signal, (c) reconstruction error.

two components are 4096 samples and 2048 samples, respectively. Both components have a peak amplitude of 0.5, so that the multi-component signal has unit peak amplitude. This signal was processed with the multi-component paradigm shown in Figure 2. The tracker correctly detected the presence of two components. Reconstruction was performed over segments of length 32 samples, with an independent initial condition being used for each component on each segment. The reconstructed signal and the reconstruction error are shown in Figures 3(b) and 3(c), respectively. The maximum reconstruction error is 0.026, less than 3% of the peak amplitude.

6 Concluding Remarks

In this paper we introduced, for the first time, a practical technique for computing the multi-component AM-FM representation. The approach utilizes computationally efficient localized nonlinear operators to estimate the amplitude and frequency modulations on a component-wise basis. We validated the representation by reconstructing a complicated signal from its estimated modulating functions. In treating nonstationary, locally-coherent signals, AM-FM modeling offers several advantages over traditional time-frequency distributions. The modulating functions are able to simultaneously capture both temporally and spectrally localized features of the signal structure and represent them naturally in a way that facilitates analysis and interpretation. Furthermore, the AM-FM representation tends to be smooth and efficient, making it amenable to compression.

References

[1] P. Maragos, T.F. Quatieri and J.F. Kaiser, "Speech nonlinearities, modulations, and energy operators," in *Proc. IEEE Int'l. Conf. Acoust., Speech, Signal Process.*, Toronto, Ontario, Canada, May 1991.

[2] A.C. Bovik, N. Gopal, T. Emmoth and A. Restrepo, "Localized measurement of emergent image frequencies by Gabor wavelets," *IEEE Trans. Info. Theory*, Special Issue on Wavelet Transforms and Multiresolution Signal Analysis, vol. IT-38, pp. 691-712, Mar. 1992.

[3] P. Maragos, T.F. Quatieri and J.F. Kaiser, "On separating amplitude from frequency modulations using energy operators," in *Proc. IEEE Int'l. Conf. Acoust., Speech, Signal Process.*, San Francisco, CA, May 1992.

[4] J.P. Havlicek, A.C. Bovik, and P. Maragos, "Modulation models for image processing and wavelet-based image demodulation," *Ann. Asilomar Conf. Signals, Syst., Comput.,* Pacific Grove, CA, Oct. 1992.

[5] A.C. Bovik, P. Maragos and T.F. Quatieri, "Measuring amplitude and frequency modulations in noise using multiband energy operators," *IEEE Int'l. Symp. Time-Freq. and Time-Scale Anal.*, Victoria, British Columbia, Canada, Oct. 1992.

[6] P. Maragos, J.F. Kaiser and T.F. Quatieri , "On amplitude and frequency demodulation using energy operators," *IEEE Trans. Signal Process.*, vol. SP-41, pp. 1532 - 1550, Apr. 1993.

[7] P. Maragos, J.F. Kaiser, and T.F. Quatieri, "Energy separation in signal modulations with applications to speech analysis," *IEEE Trans. Signal Process.*, vol. SP-41, pp. 3024 - 3051, Oct. 1993.

[8] A.C. Bovik, P. Maragos and T.F. Quatieri, "AM-FM energy detection and separation in noise using multiband energy operators," *IEEE Trans. Signal Process.*, Special Issue on Wavelets and Signal Processing, vol. SP-41, pp. 3245 - 3265, Dec. 1993.

[9] J.P. Havlicek and A.C. Bovik, "Multi-component AM-FM image models and wavelet-based demodulation with component tracking," in *Proc. IEEE Int'l. Conf. Image Process.*, Austin, TX, Nov. 1994.

[10] A. Papoulis, *Systems and transforms with applications in optics*, New York: McGraw-Hill, 1968.